*International Journal of Thermophysics, Vol. 4, No. 3, 1983*

# Thermophysical Properties of Liquid Copper and Aluminum

**G. R. Gathers**[1]

*Received May 3, 1983*

The electrical resistivity and equation of state of liquid copper and aluminum have been measured to temperatures of 4500 and 4000 K, respectively, using the isobaric expansion apparatus. The specific heats for the liquid are in good agreement with extrapolation of the 1973 Hultgren tables. The electrical resistivities are presented both with and without correction for thermal expansion. Both resistivity and thermal expansion results for aluminum are compared with the predictions of pseudopotential calculations. The specific volumes observed for both metals are less than those reported in the literature, apparently because of axial hydrodynamic displacement. In addition, sudden rapid acceleration in sample growth rate with a corresponding rapid rise in resistivity were observed.

**KEY WORDS:** aluminum; copper; electrical resistivity; enthalpy; high temperature; specific heat; thermal expansion.

## 1. INTRODUCTION

Thermophysical properties data for liquid copper and aluminum are of considerable importance because of the extensive use of these metals as electrical conductors. Magnetohydrodynamic (MHD) calculations require both equation of state and electrical resistivity data. To date, the available data in the literature are rather sparse because of the experimental difficulties involved. They largely consist of steady state measurements such as the pycnometer or calorimeter type. As a result, the temperature range has been restricted to values below 2000 K. In recent years dynamic methods have been developed for metals, using rapid electrical self heating and

[1] University of California, Lawrence Livermore National Laboratory, Livermore, California 94550, U.S.A.



0195-928X/83/0900-0209$03.00/0 

continuous measurement of temperature, energy input, sample size, heating current, and voltage developed across the sample. These pulse heating measurements have been hampered by the combination of low mass density and high electrical conductivity, which results in considerable sensitivity to MHD instability. Measurements on copper and aluminum have been made using the isobaric expansion apparatus (IEX) [1] at Livermore at a pressure of 0.3 GPa.

## 2. EXPERIMENTAL RESULTS

### 2.1. Sample Details

The copper samples used in this work had a purity of 99.999% and were supplied in the form of wire wound on a spool. Lengths of wire were given a tensile impulse to straighten them. Samples were then cut to the desired length and checked for uniformity before assembling them into the holder. The sample diameter was chosen to be 0.069 cm in order to reduce the heating current requirements from the capacitor bank without seriously compromising the precision of the volume measurements. In order to clamp the sample ends sufficiently it was necessary to custom machine the opening in the jaws to match the sample size and cut sample lengths such that the ends (which remain solid) were supported and could not move axially in the jaws. The aluminum samples were supplied as wire of 0.064 cm diameter, wound on a spool. The purity was 99.5%. The same straightening procedure was used. The placement of the contact probes for voltage measurements presented unusual difficulties for these metals, particularly for aluminum because of the softness of the material. Very thin gold plated molybdenum strips were used to touch the sample with a sharp edge. The distance between the contacting edges of the two probes was measured with an optical comparator. It was necessary to use a modest amount of force in setting the probes to make the assembly rugged enough for handling and pumping the cell to operating pressure. Too much force, however, would cause the sample to gradually yield and either cause MHD kink instability or loss of probe contact before the shot was fired. The latter event occurred for approximately 15% of the shots attempted.

The clamping arrangement was modified to incorporate clamping jaws attached to swivel ball joints so that the misalignments between jaws would not result in samples with a bend in them, leading to kink instability. The space consumed in the holder by the swivel balls reduced the length of sample between clamping jaws to about 1.6 cm resulting in a length to diameter ratio of 23. For shots without the swivel ball arrangement the length to diameter ratio was approximately 37.

## 2.2. Copper Results

The nature of the isobaric expansion experiment makes it much more convenient to determine measured quantities relative to specific enthalpy rather than temperature. In addition, the enthalpy is a much more reliably measured quantity than temperature. Results from the literature which use temperature as the independent variable have thus had the temperature converted to enthalpy using the 1973 Hultgren tables [2] for purposes of comparison.

For copper, the temperature measurements are shown in Fig. 1. The specific heat in the liquid is quite consistent with extrapolation of the data reported in the Hultgren tables. The curve fitted through the experimental points corresponds to

$$H\,(\mathrm{MJ}\cdot\mathrm{kg}^{-1}) = -0.22367 + 6.8142\times 10^{-4}T - 3.1631\times 10^{-8}T^2$$

$$(2000\ \mathrm{K} \leqslant T \leqslant 4500\ \mathrm{K}) \qquad (1)$$

where the reference enthalpy is that for the state at 298 K and 0.3 GPa (i.e., no correction was made for work done in pressurizing the cell). The argon calorimeter measurements of Stephens [3] and the levitation calorimetry measurements of Chaudhuri et al. [4] are shown for comparison. The

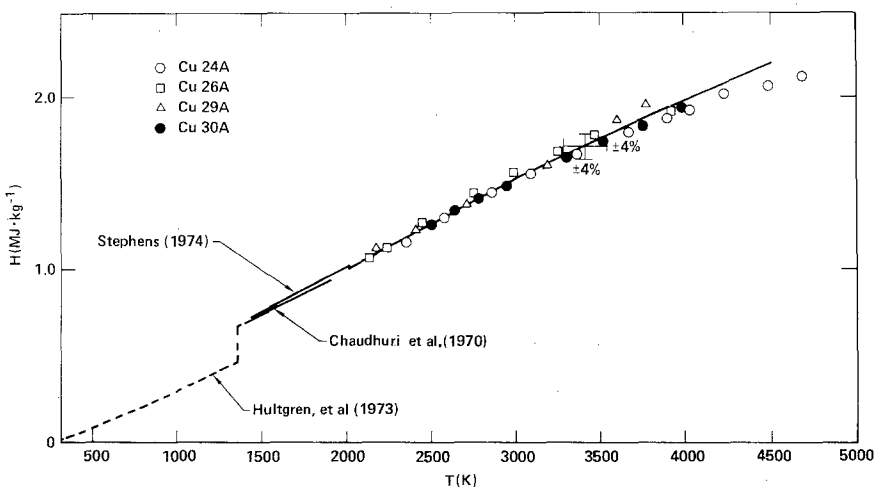


**Fig. 1.** Temperature results for copper. The dashed curve extends to 1800 K and represents the data portion of the 1973 Hultgren tables [2]. The calorimetry results of Stephens [3] and Chaudhuri et al. [4] are shown for comparison. The solid curve through the data points describes the values listed in Table I.

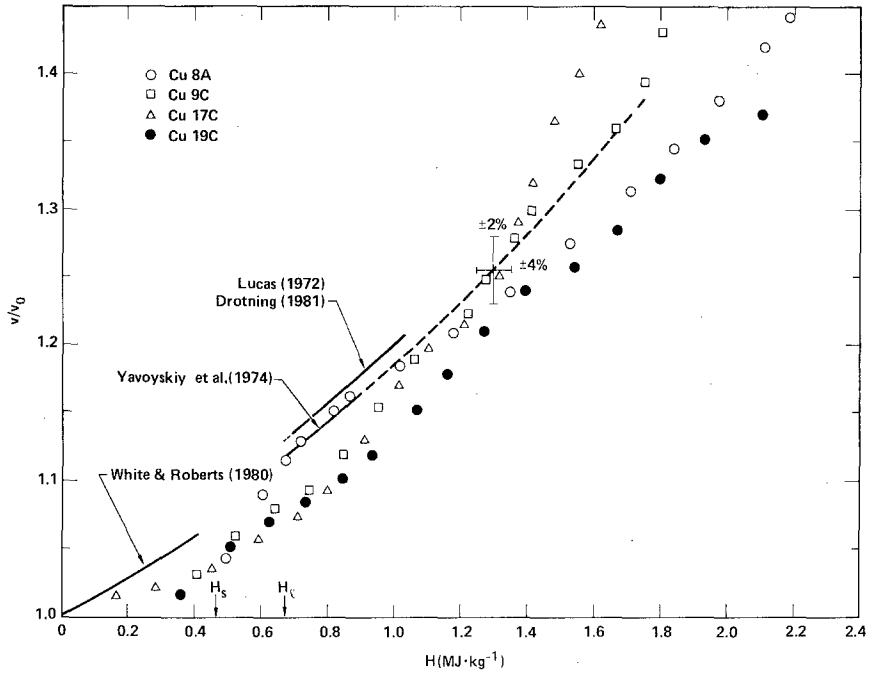


**Fig. 2.** Volume results for copper. The dashed curve describes the values in Table I and extends to the liquidus. The gamma ray transmission results of Yavoyskiy et al. [5] and those of Drotning [7] are shown with the Archimedean displacement measurements of Lucas [6]. The linear thermal expansion values of White and Roberts [10] are shown in the solid range. The enthalpies at the beginning and completion of melt are indicated according to the results of Hultgren et al. [2].

dotted curve corresponding to the Hultgren tables extends to 1800 K. Values beyond that temperature in the tables are estimates.

The specific volume data are shown in Fig. 2. The substantial scatter is expected because of the instabilities observed. The dotted curve shown is described by

$$v/v_0 = 1.0134 + 0.12091H + 5.0623 \times 10^{-2}H^2 \qquad (2)$$
$$(0.671 \text{ MJ} \cdot \text{kg}^{-1} \leqslant H \leqslant 1.75 \text{ MJ} \cdot \text{kg}^{-1})$$

Yavoyskiy et al. [5] measured density to a temperature of 1800 K using the gamma ray absorption method. Lucas [6] used the Archimedean displacement method to measure density to 1873 K. Drotning [7] used the gamma ray method to make measurements to 2000 K. The Archimedean measure-

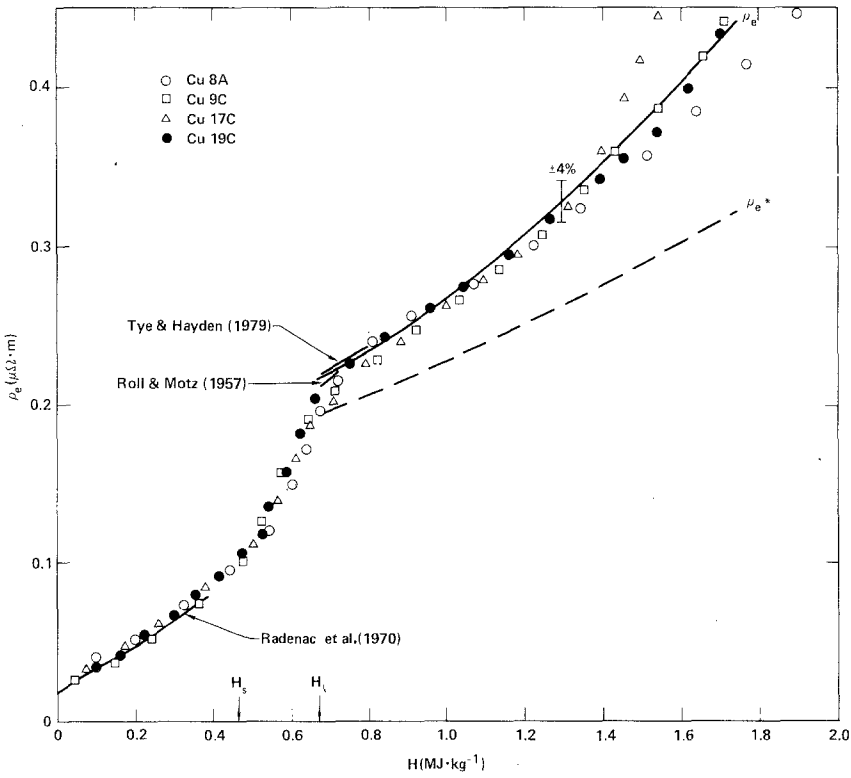


**Fig. 3.** Electrical resistivity results for copper. The solid curve through the data points describes the values in Table I. Results from the literature are shown for comparison. The dashed curve shows the result neglecting thermal expansion. The enthalpies at the beginning and completion of melt are indicated.

ments of Gomez et al. [8] and the pycnometer measurements of Ruud et al. [9] are virtually indistinguishable from the results of Drotning and Lucas. White and Roberts [10] evaluated linear thermal expansion in the solid range as part of the CODATA[2] effort. The corresponding density is shown.

Figure 3 shows the electrical resistivity data plotted against enthalpy. Tye and Hayden [11] measured electrical resistivity, using a standard four probe technique, to 1673 K. Their results are seen to be in good agreement with this work. Roll and Motz [12] and Radenac et al. [13] used magnetic deflection methods. The results of each are also shown in the figure.

[2]Committee on Data for Science and Technology (General Assembly of the International Council of Scientific Unions).

Since the scatter in the volume data were larger than has been encountered with other metals, the resistivity was also calculated using resistance ratio and the fixed room temperature geometry for each shot. A least square fit was made to the results and is described by

$$\rho_e^*(\mu\Omega \cdot \mathrm{m}) = 0.13870 + 6.5398 \times 10^{-2}H + 2.1857 \times 10^{-2}H^2 \quad (0.671\ \mathrm{MJ \cdot kg^{-1}} \leqslant H \leqslant 1.75\ \mathrm{MJ \cdot kg^{-1}}) \tag{3}$$

This gives the resistivity without correction for thermal expansion and is shown as the dashed curve in Fig. 3. For self-consistency, the final resistivity curve was obtained by multiplying Eq. (3) by Eq. (2) to give a result described by

$$\rho_e(\mu\Omega \cdot \mathrm{m}) = 0.15451 + 4.4148 \times 10^{-2}H + 6.8548 \times 10^{-2}H^2 \quad (0.671\ \mathrm{MJ \cdot kg^{-1}} \leqslant H \leqslant 1.75\ \mathrm{MJ \cdot kg^{-1}}) \tag{4}$$

This is shown as the solid curve in Fig. 3. Figure 4 shows the resistivity $\rho_e$ plotted against the specific volume. The solid curve was derived from Eqs.

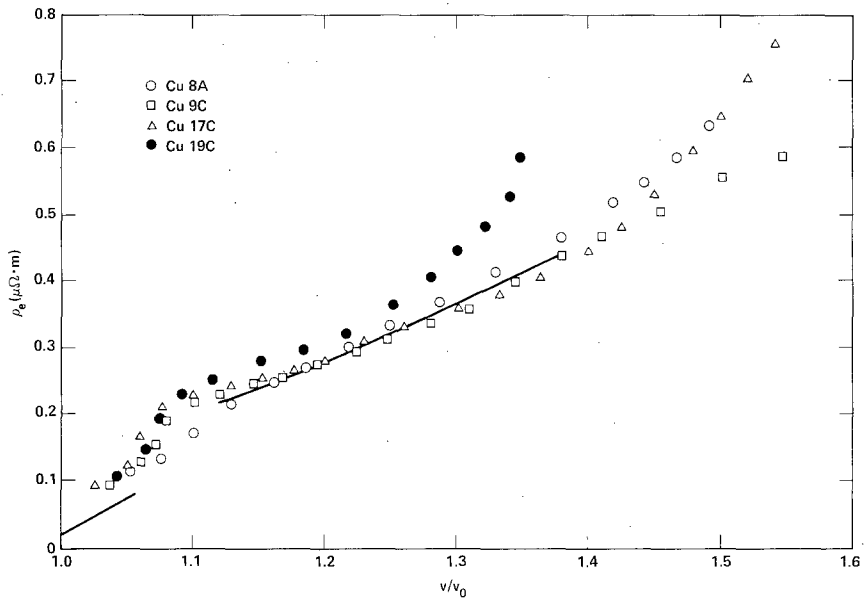


**Fig. 4.** Electrical resistivity vs volume for copper. The solid curve is represented by Eq. (5). The solid range curve corresponds to the volumes of ref. [10] and the resistivity of ref. [13].

Table I. Thermophysical Data for Copper[a]

| $T$ (K) | $H$ (MJ · kg$^{-1}$) | $v/v_0$ | $\rho_e$ ($\mu\Omega$ · m) | $\rho_e^*$ ($\mu\Omega$ · m) |
|---|---|---|---|---|
| 1356 | 0.671 | 1.117 | 0.215 | 0.192 |
| | 0.700 | 1.123 | 0.219 | 0.195 |
| | 0.800 | 1.14 | 0.234 | 0.205 |
| | 0.900 | 1.16 | 0.250 | 0.215 |
| | 1.000 | 1.185 | 0.267 | 0.226 |
| 2000 | 1.013 | 1.188 | 0.270 | 0.227 |
| 2250 | 1.149 | 1.22 | 0.296 | 0.243 |
| 2500 | 1.282 | 1.26 | 0.324 | 0.259 |
| 2750 | 1.411 | 1.29 | 0.353 | 0.275 |
| 3000 | 1.536 | 1.32 | 0.384 | 0.291 |
| 3250 | 1.657 | 1.36 | 0.416 | 0.307 |
| 3500 | 1.774 | 1.39 | 0.449 | 0.324 |
| 3750 | 1.887 | | | |
| 4000 | 1.996 | | | |
| 4250 | 2.101 | | | |
| 4500 | 2.202 | | | |

[a] $v_0 = 1.120 \times 10^{-4}$ m$^3$ · kg$^{-1}$. Reference state: 298 K, 0.3 GPa.

(2) and (4) for the appropriate range of enthalpies and is described by

$$\rho_e(\mu\Omega \cdot \mathrm{m}) = -8.7008 \times 10^{-2} - 0.20960\,(v/v_0) + 0.42952\,(v/v_0)^2 \qquad (1.12 \leqslant v/v_0 \leqslant 1.38) \tag{5}$$

The results for copper are summarized in Table I.

### 2.3. Aluminum Results

Figure 5 shows the temperature data for aluminum. As for copper, the specific heat in the liquid is quite consistent with the extrapolation in the Hultgren tables. The solid curve is described by

$$H\ (\mathrm{MJ} \cdot \mathrm{kg}^{-1}) = 4.8910 \times 10^{-2} + 1.0704 \times 10^{-3}T + 2.3084 \times 10^{-8}T^2 \qquad (933\ \mathrm{K} \leqslant T \leqslant 4000\ \mathrm{K}) \tag{6}$$

where the reference state is that for 298 K and 0.3 GPa. Figure 6 shows the specific volume data. The solid curve is described by

$$v/v_0 = 1.0205 + 8.3779 \times 10^{-2}H + 4.9050 \times 10^{-3}H^2 \qquad (1.07\ \mathrm{MJ} \cdot \mathrm{kg}^{-1} \leqslant H \leqslant 6.0\ \mathrm{MJ} \cdot \mathrm{kg}^{-1}) \tag{7}$$

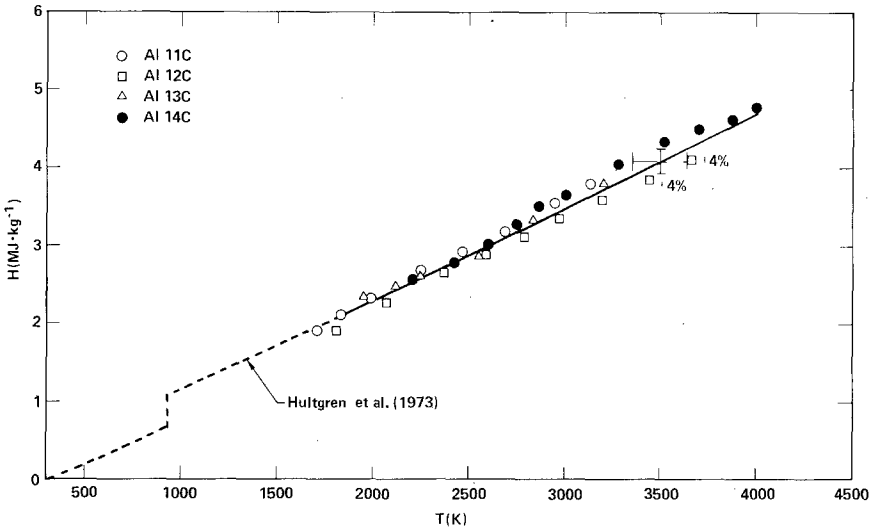


**Fig. 5.** Temperature results for aluminum. The dashed curve represents the data portion of the Hultgren tables [2]. The values in Table II represent a combination of the data portion of the Hultgren tables and the solid curve fitted through the data points.

Gol'tsova [14] used a dilatometric method to determine the volumetric expansion of the liquid over the temperature range 1273 to 1773 K. Wilson [15] used a novel method of igniting small particles of aluminum in an $O_2/Ar$ gas mixture with a laser beam while taking motion pictures of the combustion and observing the increase in droplet diameter. Temperature was not measured directly, but inferred from the Clapeyron equation. The observed expansions of Gol'tsova and Wilson are substantially larger than those observed with the IEX measurements.

The resistivity results are shown in Fig. 7 as a function of enthalpy. The solid curve marked $\rho_e$ was chosen to represent the data and is described by

$$\rho_e(\mu\Omega \cdot m) = 0.15916 + 8.5863 \times 10^{-2}H + 8.5435 \times 10^{-3}H^2 \qquad (8)$$

$$(1.07\ \text{MJ} \cdot \text{kg}^{-1} \leqslant H \leqslant 5.0\ \text{MJ} \cdot \text{kg}^{-1})$$

As with copper, a separate analysis of each shot was made, using the resistance ratio and room temperature geometry to calculate resistivity without correction for thermal expansion. A fit made to the results is given

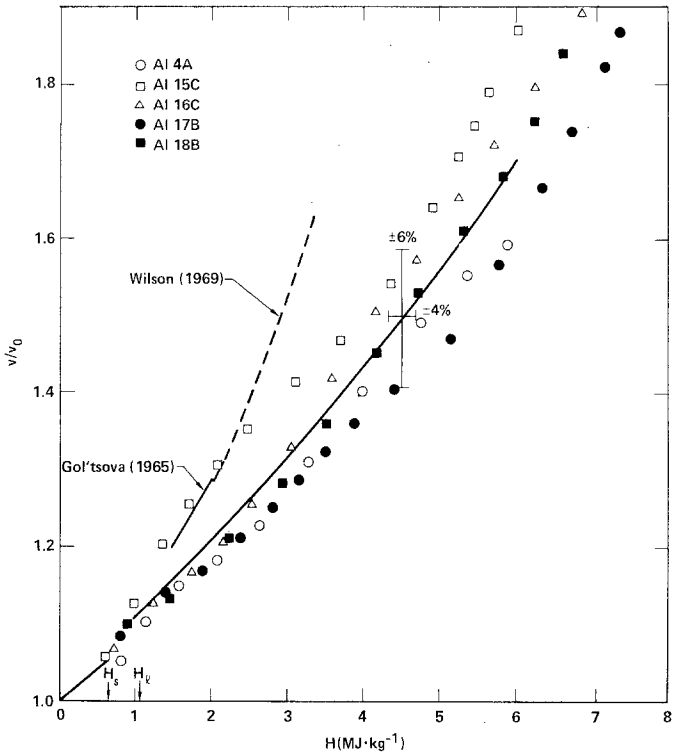


**Fig. 6.** Volume results for aluminum. The dilatometric measurements of Gol'tsova [14] and the laser combustion results of Wilson [15] are shown for comparison. The enthalpies at the beginning and completion of melt are indicated. The solid curve through the data points describes the values in Table II. The solid range curve was taken from ref. [28].

by

$$\rho_e^*(\mu\Omega \cdot \mathrm{m}) = 0.14936 + 7.9448 \times 10^{-2} H - 1.3189 \times 10^{-3} H^2 \qquad (9)$$
$$(1.07\ \mathrm{MJ} \cdot \mathrm{kg}^{-1} \leqslant H \leqslant 5.0\ \mathrm{MJ} \cdot \mathrm{kg}^{-1})$$

and is shown in the figure. Equation (8) is a fit to the results obtained by multiplying Eq. (9) by Eq. (7) in the range of overlap.

Kononenko et al. [16] measured electrical resistivity and viscosity of aluminum from melt to 1300 K using a magnetic deflection technique. They used a crucible suspended in a furnace with a superimposed magnetic field. Resistivity was determined by the amplitude of torsional deflection of the crucible and melt, while viscosity was determined from the damping of

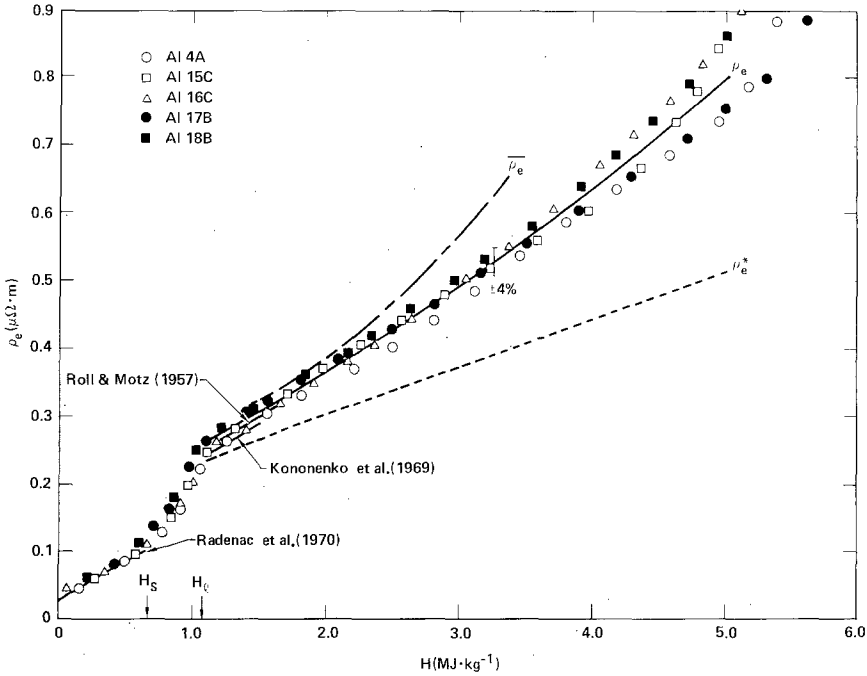


**Fig. 7.** Electrical resistivity results for aluminum. The solid curve through the data points describes the values in Table II. The curve marked $\rho_e^*$ describes the values obtained when thermal expansion corrections are not made. If the combined volume data of Gol'tsova and Wilson are used to make thermal expansion corrections to the results for $\rho_e^*$, the curve marked $\bar{\rho}_e$ results. The enthalpies at the beginning and completion of melt are indicated. Values from the literature are included for comparison.

the vibrations. Their results are shown in Fig. 7 along with the results of Roll and Motz and of Radenac et al. It is of interest to determine what resistivity would result if the resistivity $\rho_e^*$ were corrected using the volumes of Wilson and Gol'tsova. The result is shown as $\bar{\rho}_e$ in Fig. 7.

The resistivity data are shown as a function of specific volume in Fig. 8. The solid curve marked $\rho_e$ corresponds to the results of Eqs. (7) and (8). It is adequately described by

$$\rho_e(\mu\Omega \cdot \mathrm{m}) = -0.79046 + 0.74540\,(v/v_0) + 0.17556\,(v/v_0)^2 \qquad (1.12 \leqslant v/v_0 \leqslant 1.56) \tag{10}$$

The result that would be obtained using the volumes of Wilson and Gol'tsova are also shown in the figure. The results for aluminum are summarized in Table II.

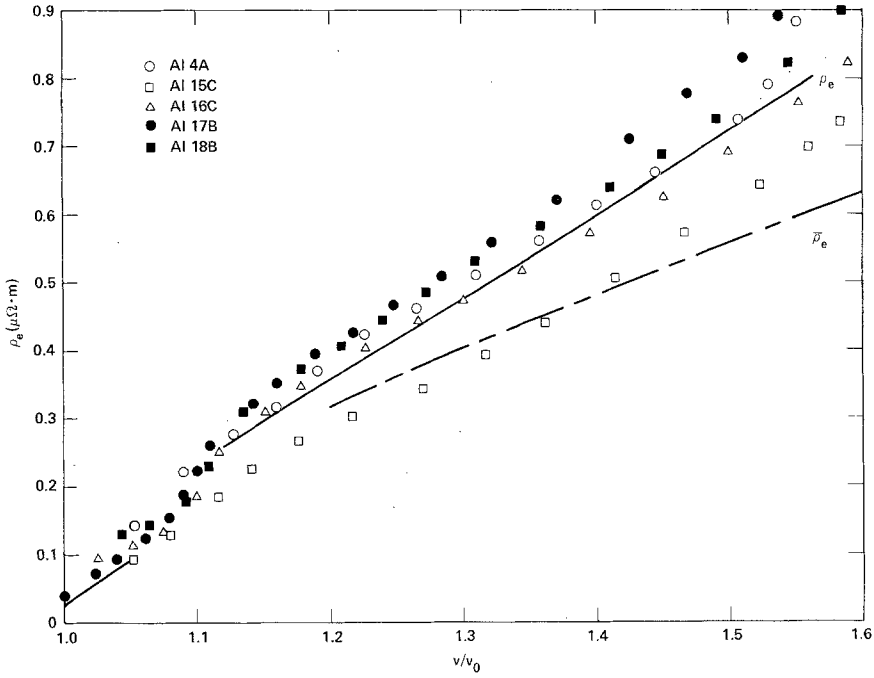


**Fig. 8.** Electrical resistivity vs volume for aluminum. The solid curve through the data points corresponds to Table II. The curve marked $\bar{\rho}_e$ corresponds to the resistance ratio data of this work corrected with the volumes of Gol'tsova and Wilson to obtain resistivity. The curve in the solid range corresponds to the resistivity of ref. [13] and the volume from ref. [28].

**Table II.** Thermophysical Data for Aluminum[a]

| $T$ (K) | $H$ (MJ · kg$^{-1}$) | $v/v_0$ | $\rho_e$ ($\mu\Omega \cdot$ m) | $\rho_e^*$ ($\mu\Omega \cdot$ m) |
|---|---|---|---|---|
| 933 | 1.068 | 1.116 | 0.233 | 0.261 |
| 1000 | 1.142 | 1.123 | 0.238 | 0.268 |
| 1500 | 1.706 | 1.18 | 0.281 | 0.331 |
| 2000 | 2.282 | 1.24 | 0.324 | 0.400 |
| 2500 | 2.869 | 1.30 | 0.366 | 0.476 |
| 3000 | 3.468 | 1.37 | 0.409 | 0.560 |
| 3500 | 4.078 | 1.44 | 0.451 | 0.651 |
| 4000 | 4.700 | 1.52 | 0.494 | 0.751 |
| | 5.000 | 1.56 | 0.514 | 0.802 |
| | 5.500 | 1.63 | | |
| | 6.000 | 1.70 | | |

[a] $v_0 = 3.706 \times 10^{-4}$ m$^3 \cdot$ kg$^{-1}$. Reference state: 298 K, 0.3 GPa.

## 3. DISCUSSION

### 3.1. Pyrometry

The melting temperatures of both copper and aluminum are below the threshold of the pyrometer used in the IEX. It is necessary to normalize results to a known temperature at a point of the data trace. A point in time near the beginning of each pyrometer trace was chosen, and the corresponding enthalpy was used with Hultgren tables to assign a temperature to the point. In each case the value chosen came from the portion of the tables that represent data rather than estimates. For the copper and aluminum results, therefore, the pyrometer was actually determining specific heat $C_p$.

### 3.2. Volume Measurements

The volumes measured for both copper and aluminum are less than those reported in the literature, particularly for aluminum. An effort was made to determine the cause of the discrepancy. An experimental determination of the resolution of the streak camera system was made. The optical system projects a real magnified image of the sample at the defining slit aperture of the system. A resolution chart was located at the slit and illuminated with a high intensity lamp while a streak picture was made. The chart was carefully oriented so that the bars on it were parallel to the direction of the sweep. The resolution at the plane of the slit was thus determined for the streak mode of the electronic camera. This uncertainty was then divided by the typical size of the sample image at the slit to determine the fractional uncertainty in sample diameter. The fractional uncertainty in volume ratio would be approximately twice as large since the diameter is squared to obtain volume. The resulting uncertainty in volume is $\pm 5\%$.

A dummy sample was installed in the pressure cell and steak pictures were made both for varying streak rate and varying levels of laser backlight intensity. Neither of these factors appeared to have significant influence. Films were read several times using the optical film reader to test the consistency of the results. The variation in results was on the order of 1% in volume.

Since an electronic streak camera is used, it is necessary to correct for nonlinearity of the electron beam optics in the camera. Before a shot is fired, a streak picture of the cold sample is made at the pressure chosen for the shot. This is processed in the same manner as the shot streak to determine and eliminate the apparent volume changes that actually represent camera nonlinearities. The volume corrections generated in this way are about 5%.

Since the discrepancies with the literature results are much larger, it was concluded that a real physical phenomenon was being observed. Evidently the full expansion did not develop because of expansion elsewhere. Apparent bulges were observed at the tips of either one or both of the sample clamping jaws, implying axial motion. It was not possible to determine the density of material in the bulges from the laser shadowgraph since even metal vapors would be sufficiently opaque to block the laser beam. If the bulges were liquid, the size is sufficient to account for the volume discrepancy. Blairs and Joasoo [17] have given the atmospheric pressure sound speed at melting as 4561 $m \cdot s^{-1}$ for aluminum and 3440 $m \cdot s^{-1}$ for copper. The sample lengths between the jaws were about 1.6 cm, and the heating cycle was typically about 30 $\mu$s long, so there was adequate time for such hydrodynamic behavior of the liquid metal.

As an experiment, it was decided to return to the original design of the holder to allow longer samples. A larger volume of liquid metal would result, so that material expanding at the jaw tips would have less effect on the radial expansion. As a result, both the apparent volume increased somewhat, and the scatter of results was reduced.

The longer geometry, however, placed one the clamping jaws out of the view of the shadowgraph. A number of shots were fired using Cu–Ni (15% Ni) alloy to increase the initial resistivity from 0.017 to 0.18 $\mu\Omega \cdot m$. This would reduce the heating current requirements and reduce the magnetic forces on the liquid. The samples were 0.1 cm in diameter, and the heating current density was $4.5 \times 10^6$ $A \cdot cm^{-2}$. No significant improvement in sample behavior resulted.

### 3.3. Character of the Instabilities

The reduced volumes observed have been attributed to axial movement of liquid metal. In addition, the upper limit of the data was determined by a different instability. In every case a point was reached during the heating cycle of a shot where both resistance ratio and apparent resistivity as functions of enthalpy began to rapidly increase in slope. At the same time, the streak record showed a large acceleration in sample expansion. In the case of aluminum, the enthalpy for the onset of this behavior was rather consistent, occurring at about 4.5–5 $MJ \cdot kg^{-1}$. For copper it was rather less consistent. The behavior is rather like that described by Lebedev [18]. The heating rate was varied somewhat but with little noticeable result. The design of the capacitor bank used in the IEX limits the range of heating rates that may be used. The current density also varies during the heating cycle as a result of the sample expansion and the rise of the current pulse. The maximum value occurs near the peak of the current

pulse. Copper shot 8 had a heating rate of about 0.3 $MJ \cdot kg^{-1} \cdot \mu s^{-1}$ while shots 9, 17, and 19 had a heating rate of about 0.1 $MJ \cdot kg^{-1} \cdot \mu s^{-1}$.

For shot 8 the maximum current density was $\sim 10^7$ $A \cdot cm^{-2}$, while for shot 9 it was $8.6 \times 10^6$ $A \cdot cm^{-2}$. For shots 17 and 19 the maximum current density was $8 \times 10^6$ $A \cdot cm^{-2}$. The heating rate for aluminum ranged from 0.8 to 1.0 $MJ \cdot kg^{-1} \cdot \mu s^{-1}$. The maximum current density ranged from $5.9 \times 10^6$ $A \cdot cm^{-2}$ for shot 15 to $6.9 \times 10^6$ $A \cdot cm^{-2}$ for shot 4. These current densities correspond to the range described by Lebedev.

Young and Alder [19] used a hard sphere van der Waals model to predict a critical pressure of 0.83 GPa and a critical volume of $2.74 \times 10^{-3}$ $m^3 \cdot mol^{-1}$ for copper. This volume corresponds to $v_c/v_0 = 3.86$. Their boiling line is shown in Fig. 9 along with the melting transition and the IEX track for this work. The end of the track corresponds to the onset of the sudden rise in resistivity and volume. Kolgatin and Khachatur'yants [20]

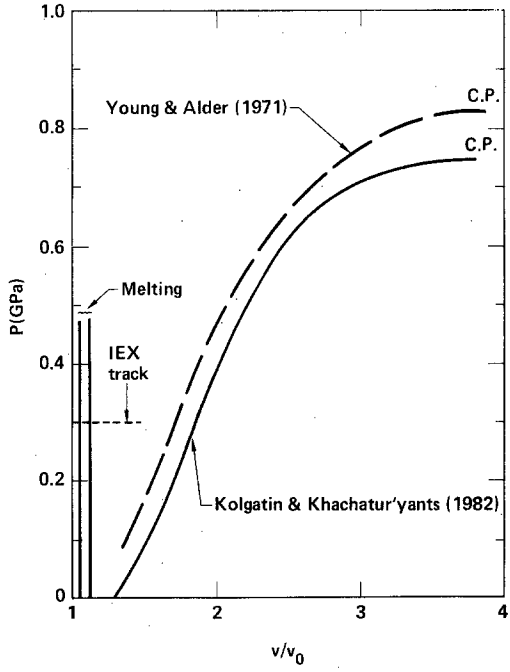


**Fig. 9.** Pressure vs volume plane for copper. The critical points and boiling curves of Young and Alder [19] and of Kolgatin and Khachatur'yants [20] are shown along with the melting transition and the IEX track used in this work. The end of the track corresponds to the onset of sudden rapid growth in sample diameter and rapidly increasing resistivity.

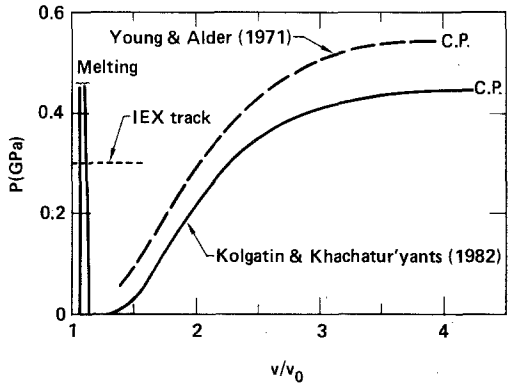


**Fig. 10.** Pressure vs volume plane for aluminum. The critical points and boiling curves of Young and Alder [19] and of Kolgatin and Khachatur'yants [20] are shown along with the melting transition. The IEX track ends at the onset of sudden rapid growth in sample diameter and resistivity.

made a fit to the critical point data in the review by Fortov et al. [21] and other standard thermophysical data to give an interpolation equation of state. Their boiling line is also shown. It appears unlikely that the instability observed is caused by the onset of boiling.

For aluminum, Young and Alder predicted a critical pressure of 0.546 GPa and a critical volume of $3.91 \times 10^{-5}$ $m^3 \cdot mol^{-1}$ corresponding to $v_c/v_0 = 3.93$. Their boiling line is shown in Fig. 10 along with the corresponding results of Kolgatin and Khachatur'yants, the melting transition, and the IEX track ending at the onset of sudden growth in resistivity and volume. Again, boiling appears to be an unlikely mechanism for the instability. In conclusion, the mechanism remains unexplained.

### 3.4. Electrical Resistivity

Aluminum is considered to be a simple nearly free electron metal which provides a useful test for theory. The thermophysical properties of liquid aluminum near normal density have been calculated by Jones [22] using pseudopotential theory. He used the Harrison pseudopotential [23] with a Geldart–Vosko dieletric constant [24, 25] and a set of parameters fitted to reproduce the experimental data for the crystal binding energy and compressibility at 0.1 MPa and 0 K. We modified his potential slightly to fit the pressure at the normal melting point. The parameters in terms of Jones' notation are $\beta = 42.9$ and $r_c = 0.298$. The thermodynamic properties

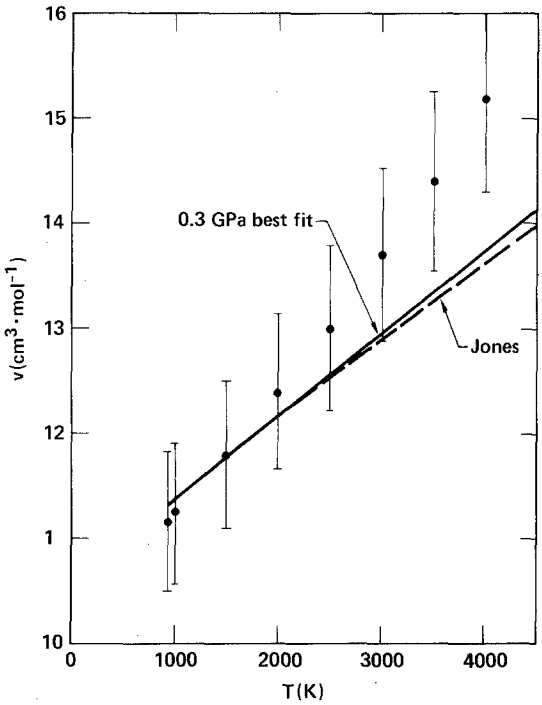


**Fig. 11.** Thermal expansion of aluminum. The points correspond to the values in Table II with ±6% error bars. The dashed curve corresponds to calculations of Jones [22] with the pseudopotential slightly altered to fit the pressure at the normal melting point. The parameters in Jones' notation are $\beta = 42.9$ and $r_c = 0.298$. The solid curve corresponds to $\beta = 46.7$ and $r_c = 0.3024$. These values give agreement with low temperature compressibility and normal liquid properties (see text).

were calculated by minimizing the Helmholtz free energy with respect to the hard sphere packing fraction and taking the appropriate derivatives of the free energy to obtain pressure and energy. In these calculations, a soft sphere rather than a hard sphere reference entropy was used [26]. The sensitivity of the results to the potential was studied by varying the parameters to $\beta = 46.7$ and $r_c = 0.3024$, while retaining the fit to normal liquid properties and the low temperature compressibility. The results are shown, respectively, as the dashed and solid curves and are compared with the experimental data for volume versus temperature in Fig. 11, and resistivity versus volume in Fig. 12. The resistivity was calculated by the method of Ashcroft and Lekner [27]. The predicted electrical resistivities are in reasonably good agreement with the measurements, but the model does less well in predicting the expansion data.

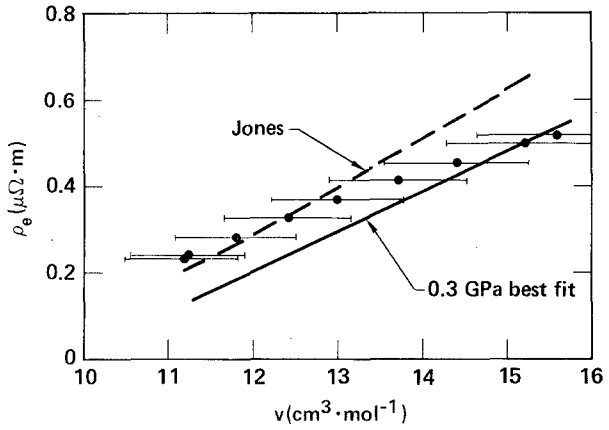


**Fig. 12.** Electrical resistivity of aluminum. The points correspond to the values in Table II with ±6% error bars. The dashed curve corresponds to calculations of Jones [22] with the pseudopotential slightly altered to fit the pressure at the normal melting point. The parameters in Jones' notation are $\beta = 42.9$ and $r_c = 0.298$. The solid curve corresponds to $\beta = 46.7$ and $r_c = 0.3024$. These values give agreement with low temperature compressibility and normal liquid properties (see text).

## 4. SUMMARY

The electrical resistivity and equation of state for liquid copper and aluminum have been measured to temperatures of 4500 and 4000 K, respectively. The specific heats are in good agreement with extrapolation of the 1973 Hultgren tables. The specific volumes observed for copper are somewhat less than those observed in other work and show unusual scatter, apparently because of axial motion of the liquid metal. The specific volumes for aluminum are quite substantially less than those reported in the literature. Electrical resistivities are reported both with and without correction for thermal expansion. Sudden rapid acceleration in sample growth rate with a corresponding rapid rise in the apparent electrical resistivity was also observed. These determined the upper bounds of the data. The exact nature of this instability is unidentified, but it appears unlikely to be related to the onset of boiling. The resistivity and thermal expansion results for aluminum were compared with the predictions of pseudopotential calculations.

## ACKNOWLEDGMENTS

This work was performed under the auspices of the U.S. Department of Energy by Lawrence Livermore National Laboratory under contract

W-7405-Eng-48. The author wishes to thank Marvin Ross for the pseudopotential calculations in aluminum.

## REFERENCES

1. G. R. Gathers, J. W. Shaner, and R. L. Brier, *Rev. Sci. Instrum.* **47**:471 (1976).
2. R. Hultgren, P. D. Desai, D. T. Hawkins, M. Gleiser, K. K. Kelley, and D. D. Wagman, *Selected Values of the Thermodynamic Properties of the Elements* (American Society for Metals, Metals Park, Ohio, 1973).
3. H. P. Stephens, *High Temp. Sci.* **6**:156 (1974).
4. A. K. Chaudhuri, D. W. Bonnell, L. A. Ford, and J. L. Margrave, *High Temp. Sci.* **2**:203 (1970).
5. V. I. Yavoyskiy, A. A. Ezhov, V. F. Kravchenko, V. S. Uskov, Yu I. Nebosov, Yu A. Chernov, and G. A. Dorofeyev, *Russ. Metall.* **1974/4**:44 (1974).
6. L. D. Lucas, *Mem. Sci. Rev. Metall.* **69**:395 (1972).
7. W. D. Drotning, *High Temp.-High Press.* **13**:441 (1981).
8. M. Gomez, L. Martin-Garin, H. Ebert, P. Bedon, and P. Desre, *Z. Metallkd.* **67**:131 (1976).
9. C. O. Ruud, M. T. Hepworth, and J. M. Fernandez, *Metall. Trans.* **6B**:351 (1975).
10. G. K. White and R. B. Roberts, *High Temp.-High Press.* **12**:311 (1980).
11. R. P. Tye and R. W. Hayden, *High Temp.-High Press.* **11**:597 (1979).
12. A. Roll and H. Motz, *Z. Metallkd.* **48**:272 (1957).
13. A. Radenac, M. Lacoste, and C. Roux, *Rev. Int. Hautes Temp. Refract.* **7**:389 (1970).
14. E. I. Gol'tsova, *High Temp. (USSR)* **3**:438 (1965).
15. R. P. Wilson, Jr., *High Temp. Sci.* **1**:367 (1969).
16. V. I. Kononenko, S. P. Yatsenko, G. M. Rubinshtein, and I. M. Privalov, *High Temp. (USSR)* **7**:243 (1969).
17. S. Blairs and U. Joasoo, *J. Inorg. Nucl. Chem.* **42**:1555 (1980).
18. S. V. Lebedev, *High Temp. (USSR)* **17**:222 (1980).
19. D. A. Young and B. J. Alder, *Phys. Rev.* **A3**:364 (1971).
20. S. N. Kolgatin and A. V. Khachatur'yants, *High Temp. (USSR)* **20**:380 (1982).
21. V. E. Fortov, A. N. Dremin, and A. A. Leont'ev, *High Temp. (USSR)* **13**:984 (1975).
22. H. D. Jones, *Phys. Rev.* **A8**:3215 (1973).
23. W. A. Harrison, *Pseudopotentials in the Theory of Metals* (Benjamin, New York, 1966).
24. D. J. W. Geldart and S. H. Vosko, *Can. J. Phys.* **44**:2137 (1966).
25. D. J. W. Geldart and S. H. Vosko, *Can. J. Phys.* **45**:2229(E) (1967).
26. M. Ross, H. E. DeWitt, and W. B. Hubbard, *Phys. Rev.* **A24**:1016 (1981).
27. N. W. Ashcroft and J. Lekner, *Phys. Rev.* **145**:83 (1966).
28. Y. S. Touloukian, R. K. Kirby, R. E. Taylor, and P. D. Desai, *Thermophysical Properties of Matter, Vol. 12 (Thermal Expansion)* (IFI/Plenum, New York, 1976).